PERFORMANCE ANALYSIS AND SIMULINK MODELING OF VERSATILE ADJUSTABLE SPEED TSCAOI INDUCTION GENERATOR

SUGUNAKAR MAMIDALA
M.Tech, Assoc. Professor
sugunakar1222@gmail.com

NAVEEN KUMAR D
M.Tech, Assistant Professor,
navinmudiraj@gmail.com

DR.KWAJA MOINUDDIN SYED
Principal,scient engineering college

ABSTRACT

Enormous advantages of induction motor (IM) like their relative cheapness, low maintenance and high reliability for industrial use has been simulated for over the years. This paper presents a novel fuzzy logic controller for cage induction generator (CIG) and presents a mathematical model, through which its behavior can be accurately predicted and performance can be improved with fuzzy controller. The inputs to the fuzzy logic controller are the linguistic variables of speed error and change of speed error, while the output is change in switching control frequency of the voltage source inverter. The two-series-connected-and-one isolated (TSCAOI) phase winding configuration magnetically decouples the two sets of windings, enabling independent control.The proposed generator system employs a three-phase cage induction machine and generates single-phase and constant-frequency electricity at varying rotor speeds without an intermediate inverter stage excitation to the isolated single winding at any frequency of generation. With low cost the proposed generator can be easily implemented. It can be used for both energy storage and retrieval through its excitation winding, and it is an ideal candidate for small-scale renewable energy applications. A dynamic mathematical model, which accurately predicts the improved behavior of the proposed generator from conventional PI controller, is also presented and implemented in MATLAB/Simulink.

I.INTRODUCTION

An induction motor being rugged, reliable, and relatively inexpensive makes it more preferable in most of the industrial drives. They are mainly used for constant speed applications because of unavailability of the variable-frequency supply voltage [1]. But many applications are in need of variable speed operations.

Induction generators have been also employed to generate single-phase electricity, particularly for standalone or residential use [4] and [5]. In [7] and [8], a self-excited and self-regulated single-phase induction generator has been reported for the generation of single-phase electricity. In contrast, the analysis of the self-excitation of a dual-winding induction generator has been presented in [21]. This paper, which uses a single-phase cage induction machine with an auxiliary winding, has been extended by connecting an inverter to the auxiliary winding to achieve more flexibility in power control [22]. All these reported schemes employed a single-phase induction generator and an auxiliary winding in some cases or a three phase induction generator to generate single-phase electricity at constant or above synchronous speed.

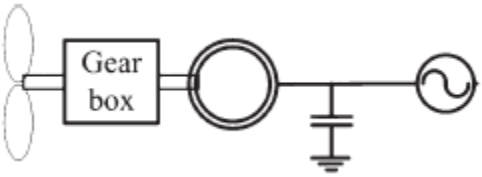

Fixed speed cage induction generator

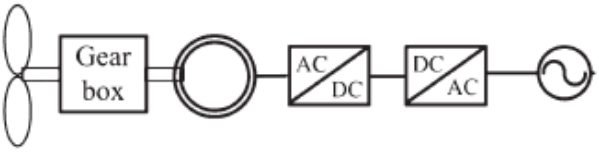

Variable speed cage induction generator

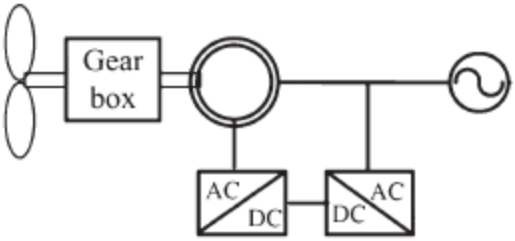

Variable speed doubly-fed induction generator

Fig.1. Typical induction generator systems used in wind turbines.

The schemes illustrated in Fig. 1, fixed-speed cage three phase induction generators are well known for their simplicity and low cost and operated at constant rotor speed to generate electricity at constant frequency for both direct grid integration and standalone operation. Usually, they are excited through a bank of capacitors and are incapable of tracking maximum power that is available from the wind turbine when operated at constant speed [4]–[6]. Therefore, in order to extract maximum energy under varying wind speed conditions, an intermediate power conversion stage, comprising an alternating-current (ac)/direct-current (dc) and dc/ac back-to-back converter configuration, is employed between the generator and the grid or the load [7]–[15]. The intermediate stage allows for the variable-speed operation of the generator, but it essentially requires to be rated for the same or a fraction (in the case of doubly fed induction generators) of the power level of the generator itself. Thus, such an intermediate stage is often found to be economically unjustifiable for some applications, particularly at micro power levels.

In this work, the conventional PI controller has been replaced by a fuzzycontroller (FC). The FC has been used in controller in place of conventional PI controller for improving the dynamic performance. The FC is basically nonlinear and adaptive in nature. The results obtainedthrough FC are superior in the cases where the effects of parameter variation of controller are alsotaken into consideration. The FC is based on linguistic variable set theory and does not require amathematical model. Generally, the input variables are error and rate of change of error. If the erroris coarse, the FC provides coarse tuning to the output variable and if the error is fine, it provides fine tuningto the output variable.

In contrast with single-phase cage induction machines, three phase cage induction machines are less expensive and small in size for a similar power rating. According to literature, a single phase electricity generation scheme, based on a variable-speed three-phase cage induction machine without an intermediate inverter stage, is yet to be reported. This paper presents a novel technique [23], whereby a three-phase cage induction machine can be used as a single-phase generator under both sub- and super-synchronous variable-speed conditions without an intermediate inverter stage. The technique uses one of the three windings in isolation for excitation and the remaining two, which are connected in series, as the power winding for the single-phase electricity generation. Alternatively, the two series-connected windings may be also used for excitation while the power is generated through the isolated single winding, as detailed in [24]. The three-phase cage induction machine is mathematically modeled in the proposed two-series connected- and-one-isolated (TSCAOI) phase winding configuration. The theoretical performance is investigated under varying operating conditions and compared with a prototype 2-kW single-phase electricity generator. Both simulated and experimental results are in good agreement and indicate that the machine can be operated both at sub- and super-synchronous rotor speeds to generate electricity at constant frequency. The proposed technique allows for both energy storage and retrieval through the excitation winding and is expected to gain popularity, particularly in

small-scale applications, being relatively simple and low in cost.

II.PROPOSED CAGE INDUCTION GENERATOR AND CONTROL STRUCTURE

Cage induction machines are undoubtedly the workhorse of the industry and can be still regarded as the main competitor to permanent-magnet machines. This is because they are self-starting, rugged, reliable, and efficient and offer a long trouble free working life. Of these cage induction machines, three phase machines are significantly less expensive, more efficient, and smaller in frame size in comparison with their single-phase counterpart of similar power ratings. Consequently, three-phase cage induction motors are economically more appealing and have thus become the preferred choice for numerous applications, even at derated power levels as encountered in the Steinmetz configuration [25], [26].

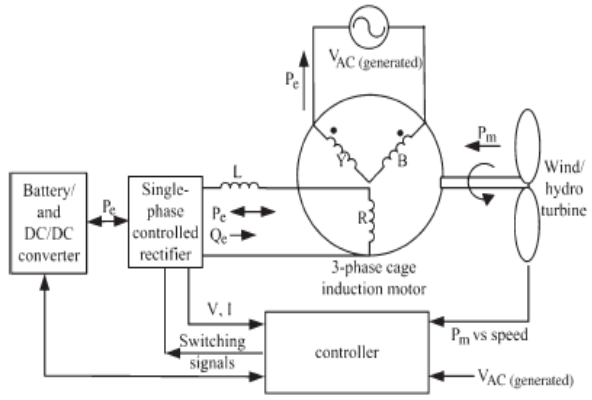

Fig. 2. Proposed generator in TSCAOI winding configuration.

The novel technique proposed in this paper also uses a three phase cage induction machine, exploiting its economical advantage, to generate single-phase electricity at variable rotor speeds without an intermediate inverter stage. The technique configures the three stator windings of the three-phase cage induction machine in a novel way to create separate or rather decoupled excitation and power windings. In this configuration, any one of the three phase windings is solely used in isolation for excitation, whereas the remaining two are connected in series to generate power at a desired frequency while the rotor is driven at any given speed. Alternatively, the machine can be also configured in such a way that the two series-connected windings provide the excitation while the single winding generates. The proposed TSCAOI winding configuration of a three-phase cage induction machine is shown in Fig. 2. As mathematically shown in the following section, the TSCAOI winding configuration magnetically decouples both excitation and power windings from each other and thus allows for independent control as in the case of a single-phase induction motor with an auxiliary winding.

In the proposed technique, excitation for the generator is provided through the single winding, which is powered by a battery using either a simple square-wave inverter or a controlled rectifier. The former is the simplest and can be operated at the desired generation frequency using a less sophisticated controller to provide the reactive-power requirement of the generator. In the latter case, as shown in Fig. 2, the system is relatively sophisticated but facilitates bidirectional power flow, allowing for both energy storage and later retrieval. The level of excitation in both cases is governed by the voltage generated in the power winding. A controller, comprising of a voltage feedback, can be employed to regulate the excitation. The controller in the simplest form may provide only the reactive power requirement of the generator (not the load) and, at a more sophisticated level, may be used to control both the active- and reactive-power flows in accordance with the phase angle and the voltage magnitude between the inverter and the excitation winding.

In the proposed technique, excitation for the generator is provided through the single winding, which is powered by a battery using either a simple square-wave inverter or a controlled rectifier. The former is the simplest and can be operated at the desired generation frequency using a less sophisticated controller to provide the reactive-power requirement of the generator. In the latter case, as shown in Fig. 2, the system is relatively sophisticated but facilitates bidirectional power flow, allowing for both energy storage and later retrieval. The level of excitation in both cases is governed by the voltage generated in the power winding. A controller, comprising of a voltage feedback, can be employed to regulate the excitation. The controller in the simplest form may provide only the reactive power requirement of the generator (not the load) and, at a more sophisticated level, may be used to control both the active- and reactive-power flows in accordance with the phase angle and the voltage magnitude between the inverter and the excitation winding.

III.MATHEMATICAL MODEL

Fig. 3(a) shows a three-phase cage induction machine configured in the proposed TSCAOI winding arrangement with no closed-loop control. For the derivation of a model, it is assumed that the "α" axis of the "$\alpha\beta$" frame is aligned with phase "a" of the stator windings, as shown in Fig. 3(b). If the rotor phase "a" is assumed to be at angle ϕr from the αaxis, rotor quantities can be transformed into the "$\alpha\beta$" frame using the following transformation:

$$[K_r] = \frac{2}{3}\begin{bmatrix} \cos(\varphi_r) & \cos\left(\varphi_r + \frac{2\pi}{3}\right) & \cos\left(\varphi_r - \frac{2\pi}{3}\right) \\ \sin(\varphi_r) & \sin\left(\varphi_r + \frac{2\pi}{3}\right) & \sin\left(\varphi_r - \frac{2\pi}{3}\right) \end{bmatrix} \quad (1)$$

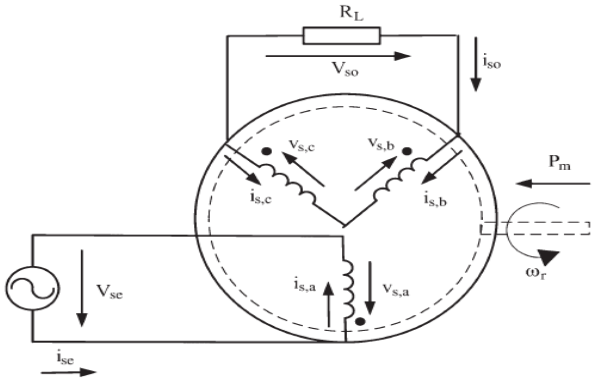

(a)

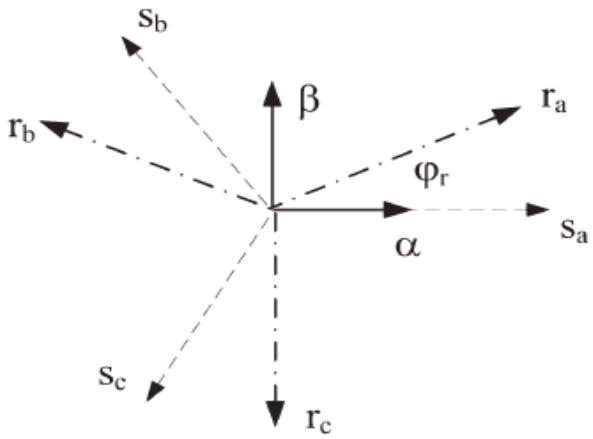

(b)

Fig.3. (a) TSCAOI model and (b) stator and rotor with respect to the "$\alpha\beta$" frame.

According to the TSCAOI configuration, the relationship between the voltages and the currents in the power and excitation windings and those in the stator-phase windings can be given by

$$[v_{s,eo}] = [Q][v_{s,abc}] \quad (2)$$

$$[i_{s,eo}] = [Q][i_{s,abc}] \quad (3)$$

Where

$$[v_{s,eo}] = \begin{bmatrix} v_{se} \\ v_{so} \end{bmatrix} [i_{s,eo}] = \begin{bmatrix} i_{se} \\ i_{so} \end{bmatrix}$$

$$[v_{s,abc}] = \begin{bmatrix} v_{sa} \\ v_{sb} \\ v_{sc} \end{bmatrix} [i_{s,abc}] = \begin{bmatrix} i_{sa} \\ i_{sb} \\ i_{sc} \end{bmatrix}$$

$$[Q] = \begin{bmatrix} 1 & 0 & 0 \\ 0 & 1 & -1 \end{bmatrix} [Q]^{-1} = [Q]^T$$

A three-phase cage induction machine can be represented in the "abc" frame by the following standard equations:

$$[v_{s,abc}] = [R_s][i_{s,abc}] + p\{[L_s][i_{s,abc}]\}$$

$$+p\{[L_{sr}][i_{r,abc}]\}(4)$$

$$[V_{r,abc}] = [R_r][i_{r,abc}] + p\{[L_{sr}]^T[i_{s,abc}]\}$$

$$+p\{[L_r][i_{r,abc}]\}(5)$$

where p is the differential operator, [*Vr*,abc] and [*Ir*,abc] are defined according to [*Vs*,abc] and [*Is*,abc], respectively, [*Vr*,abc] = 0 for cage machines, and

$$[R_s] = \begin{bmatrix} r_s & 0 & 0 \\ 0 & r_s & 0 \\ 0 & 0 & r_s \end{bmatrix} [R_r] = \begin{bmatrix} r_r & 0 & 0 \\ 0 & r_r & 0 \\ 0 & 0 & r_r \end{bmatrix}$$

$$[L_s] = \begin{bmatrix} (L_{1s} + L_{ms}) & -L_{ms}/2 & -L_{ms}/2 \\ -L_{ms}/2 & (L_{1s} + L_{ms}) & -L_{ms}/2 \\ -L_{ms}/2 & -L_{ms}/2 & (L_{1s} + L_{ms}) \end{bmatrix}$$

$$[L_r] = \begin{bmatrix} (L_{1r} + L_{mr}) & -L_{mr}/2 & -L_{mr}/2 \\ -L_{mr}/2 & (L_{1r} + L_{mr}) & -L_{mr}/2 \\ -L_{mr}/2 & -L_{mr}/2 & (L_{1r} + L_{mr}) \end{bmatrix}$$

$$[L_{sr}] = L_{ms} \begin{bmatrix} \cos(\varphi_r) & \cos\left(\varphi_r + \frac{2\pi}{3}\right) & \cos\left(\varphi_r - \frac{2\pi}{3}\right) \\ \cos\left(\varphi_r - \frac{2\pi}{3}\right) & \cos(\varphi_r) & \cos\left(\varphi_r + \frac{2\pi}{3}\right) \\ \cos\left(\varphi_r + \frac{2\pi}{3}\right) & \cos\left(\varphi_r - \frac{2\pi}{3}\right) & \cos(\varphi_r) \end{bmatrix}$$

In these equations, parameters r_s, r_r, L_{ls}, L_{ms}, L_{lr}, L_{mr}, and L_{sr} are the stator resistance, the rotor resistance, the stator leakage, the stator magnetization, the rotor leakage, the rotor magnetization, and the stator-to-rotor mutual inductance referred to the stator side, respectively. The stator and rotor parameters in the "abc" frame can be now transformed into the "eo" and "*αβ*" frames, respectively, i.e.,

$$[v_{s,eo}] = [Q][R_s][Q]^{-1}[i_{s,eo}] + [Q]p\{[L_s][Q]^{-1}[i_{s,eo}]\}$$

$$+[Q]p\{[L_{sr}][K_r]^{-1}[i_{r,\alpha\beta}]\}(6)$$

$$[v_{r,\alpha\beta}] = [K_r][R_r][K_r]^{-1}[i_{r,\alpha\beta}] + [K_r]p\{[L_{sr}]^T[Q]^{-1}[i_{s,eo}]\}$$

$$+[K_r]p\{[L_r][K_r]^{-1}[i_{r,\alpha\beta}]\}(7)$$

After lengthy manipulations with appropriate substitutions, (6) and (7) can be rewritten in the following form:

$$[v_{s,eo}] = r_s \begin{bmatrix} 1 & 0 \\ 0 & 2 \end{bmatrix} [i_{s,eo}] + \begin{bmatrix} L_{ls} + L_{ms} & 0 \\ 0 & 2L_{ls} + 3L_{ms} \end{bmatrix} p[i_{s,eo}] + \frac{3}{2} L_{ms} \begin{bmatrix} 1 & 0 \\ 0 & \sqrt{3} \end{bmatrix} p[i_{s,\alpha\beta}] \quad (8)$$

$$0 = L_{ms} w_r \begin{bmatrix} 0 & \sqrt{3} \\ -1 & 0 \end{bmatrix} [i_{s,eo}] + L_{ms} \begin{bmatrix} 1 & 0 \\ 0 & \sqrt{3} \end{bmatrix} p[i_{s,eo}] r_r [i_{r,\alpha\beta}] + \left(L_{lr} + \frac{3}{2} L_{ms}\right) w_r \begin{bmatrix} 0 & 1 \\ -1 & 0 \end{bmatrix} [i_{r,\alpha\beta}]$$

$+\left(L_{lr}+\frac{3}{2}L_{ms}\right)p[i_{r,\alpha\beta}]$(9)

Where ωr is the rotor speed in electrical radians per second.

From (8) and (9), it is evident that the excitation and power windings are decoupled. To complete the machine model, it is necessary to select state variables and derive the appropriate equations for integration. In this case, the elements of the machine current vector are chosen as the state variables.

Equation (10) shows the state space model using the winding currents as the phase vector, as derived from (8) and (9), i.e.,

$$p[i] = [A][i] + [B][i] \quad (10)$$

Where the parameters are shown at the bottom of the page.

The electromagnetic torque of the machine can be derived from

$$T_e = \frac{P}{2}\left[i_{s,abc}\right]\frac{\partial}{\partial \varphi_r}\left\{\left[L_{sr}\right]\left[i_{r,abc}\right]\right\} \quad (11)$$

Where*P* denotes the number of poles. Equation (11) in "abc" quantities is transformed into the "eo" and "$\alpha\beta$" frames and can be given by

$$T_e = \frac{P}{2}L_M(\sqrt{3}i_{so}i_{r\alpha} - i_{se}i_{r\beta}) \quad (12)$$

Equation (12) represents the torque components due to both load and excitation currents. At the steady state, the torque given in (12) is equal to the turbine torque. The equation of the motion of the generator is given by

$$P\omega_r = \frac{P}{2}\frac{1}{J}(T_P - T_e) \quad (13)$$

Where *J* (in kg · m2) is the inertia and *Tp*(in nanometers) is the torque of the prime mover.

IV.CONTROL OF THE GENERATOR

Both the behavior and the performance of the machine in the proposed TSCAOI generator configuration are investigated through simulations, implementing the previously mentioned mathematical model in MATLAB/Simulink using a 2-kW prototype generator. This information was used to develop the closed-loop controller, as shown in Fig. 4. The single-phase output voltage *VO* is converted to a root-mean-square (RMS) value and compared with the desired output voltage, in this case, 230-V RMS. The voltage error is fed to a proportional–integral (PI) controller in conventional method.

The disadvantage of PI controller is its inability to react to abrupt changes in the error signal, ε, because it is only capable of determining the instantaneous value of the error signal without considering the change of the rise and fall of the error, which in mathematical terms is the derivative of the error denoted as Δε. To solve this problem by using Fuzzy logic controller.

FUZZY LOGIC CONTROLLER

FLC contains three basic parts: Fuzzification, Base rule, and Defuzzification. FLC has two inputs which are: error and the change in error, and one output. The Fuzzy Controller structure is represented in fig.4. The role of each block is the following:

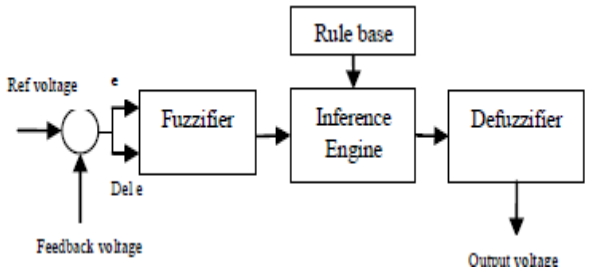

Fig 4: The general structure of Fuzzy Logic

	NL	NM	NS	ZE	PS	PM	PL
NL	PL	PL	PL	PL	PM	PS	ZE
NM	PL	PL	PM	PM	PS	ZE	NS
NS	PL	PM	PS	PS	NS	NM	NL
ZE	PL	PM	PS	ZE	NS	NM	NL
PS	PL	PM	PS	NS	NS	NM	NL
PM	PM	ZE	NS	NM	NM	NL	NL
PL	ZE	NS	NM	NL	NL	NL	NL

Controller

Fuzzifierconverts a numerical variable into a linguistic label.. In a closed loop control system, the error (e) between the reference voltage and the output voltage and the rate of change of error (del e) can be labeled as zero (ZE), positive small (PS), negative small (NS), etc. In the real world, measured quantities are real numbers (crisp). The FLC takes two inputs, i.e., the error and the rate of change of error. Based on these inputs, The FLC takes an intelligent decision on the amount of field voltage to be applied which is taken as the output and applied directly to the field winding of generator. Triangular membership functions were used for the controller.

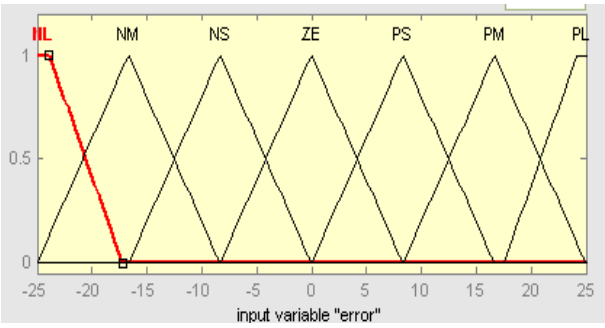

Fig 5. Membership function of voltage

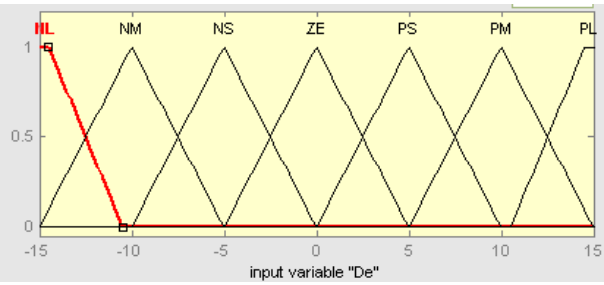

Fig 6. Membership function of voltage error

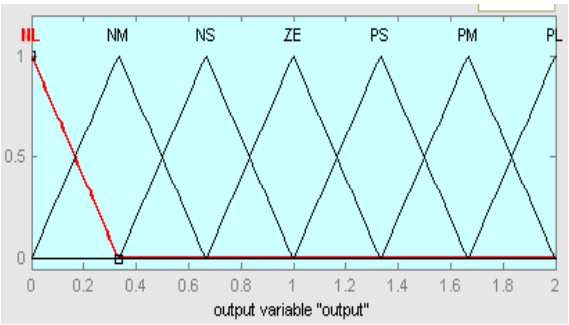

Fig 7. Membership function of output field voltage

Rule base stores the data that defines the input and the output fuzzy sets, as well as the fuzzy rules that describe the control strategy. Mamdani method is used in this paper. Seven membership functions were used leading to 49 rules in the rule base.

Table 1: Rule base for fuzzy controller

Inference engine applies the fuzzy rules to the input fuzzy variables to obtain the output values. Defuzzifier achieves output signals based on the output fuzzy sets obtained as the result of fuzzy reasoning. Centroid defuzzifier is used here.

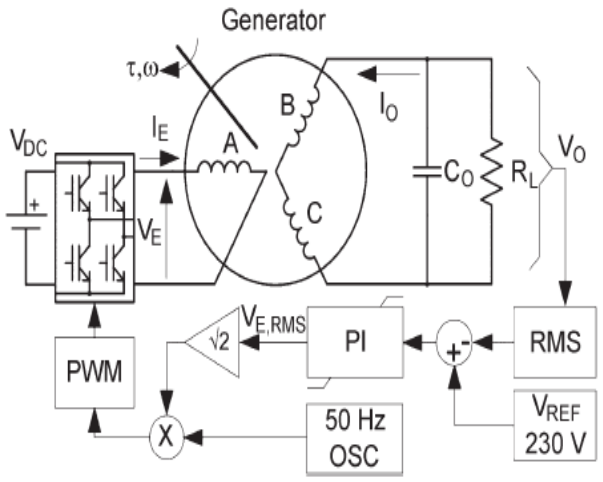

Fig.8. Control block diagram.

V.SIMULATION RESULTS

In order to verify the controller of the proposedconcept, a prototype 2-kW generator was built using3-kW 400-V cage induction machine.An extensive simulation study is carried out using MATLAB/Simulink as shown in fig.9. Induction motor using a variable-speed drive (VSD) to emulate the variable wind conditions. The controller in Fig. 8 was implemented,to supply power to a standalone and electronic load at 230 V/50 Hz under varying rotor speeds. A 30-μF capacitor, shown as C_0 in Fig. 8,was employed to reduce the reactive-power requirement of theexcitation source and to keep the magnitude of the excitationcurrent below the rated value of the machine.

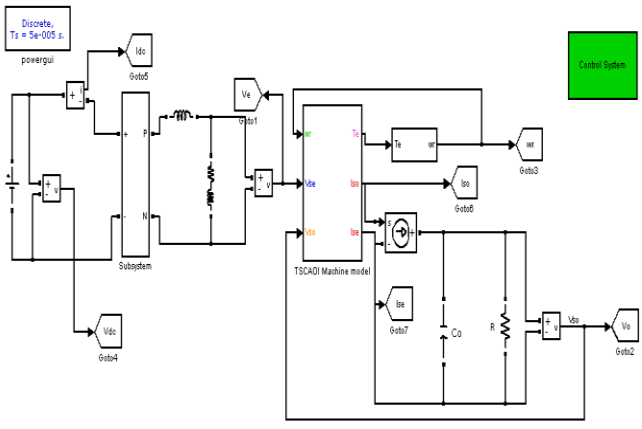

Fig.9 simulation diagram of proposed system

Fig. 10 shows the variation of the excitation current for different rotor speeds of the generator and three different resistive loads. In all cases, the excitation control system presented in Fig. 8 is used to regulate the output voltage at 230-V RMS.

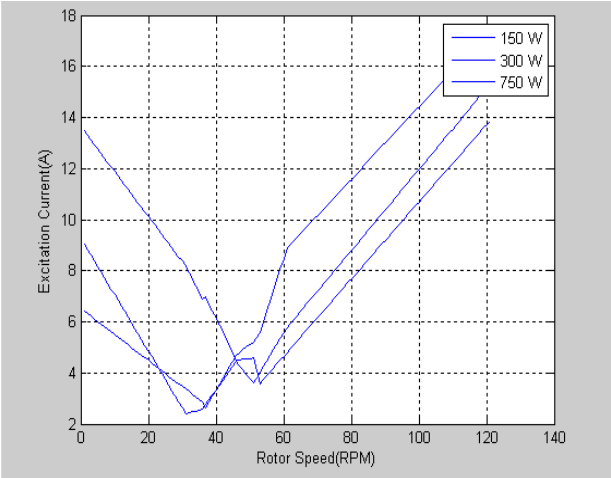

Fig.10. Excitation current for different rotor speeds and loads.

The variation of the excitation voltage versus the rotor speed is shown in Fig. 11. The impedance seen by the excitation source is complex in nature, being dependent on both the excitation frequency and the slip frequency. The slip-frequency-dependent component of the impedance changes with the rotor speed and is therefore dictated by the rotor speed and current. It appears from results that the variation of both the excitation voltage and current is largely governed by the rotor-speed-dependent impedance, and therefore, the trend in the excitation voltage variation is expected to be similar to that observed for the excitation current, as shown in Fig. 10.

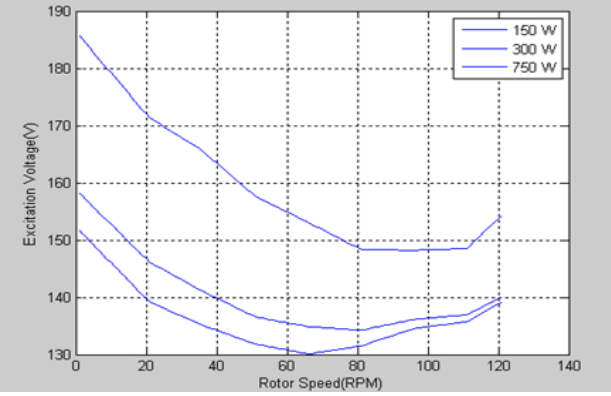

Fig.11. Excitation voltage for different rotor speeds and loads.

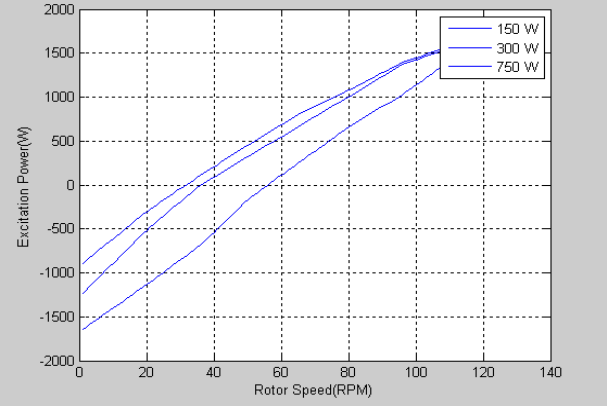

Fig.12. Excitation power for different rotor speeds and loads.

Fig. 12 demonstrates the variation of the real power of the excitation source for different rotor speeds. The negative power and the positive power indicate the power supplied and absorbed by the source, respectively. The rotor speed was simply increased or decreased by increasing or decreasing the torque setting of the VSD. It is clearly evident that, as described earlier, there is a unique rotor speed for each load at which the excitation source neither absorbs nor supplies real power but only meets the reactive-power requirement of the machine. At
this speed, both the load power and the losses of the generator are met by the turbine and thus correspond to the minimum excitation current in Fig. 10. The operation of the generator above or below this rotor speed is similar to the operation of a doubly fed induction generator in the super- or sub synchronous mode, respectively. Above this rotor speed, the turbine power is more than that is required by the load and the losses of the generator, and hence, the excess power is absorbed by the excitation source.

By adding the load power to the excitation power in Fig.12, the total real electrical power output of the generator is obtained and shown in Fig. 13 with respect to varying rotor speeds. Both the experimental and simulated results are in good agreement except for speeds below the synchronous speed of 50 Hz.

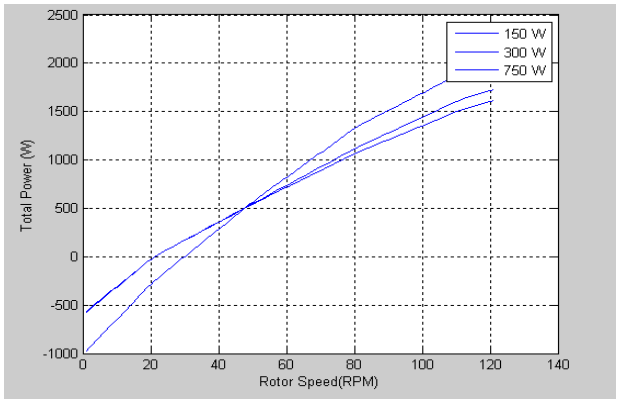

Fig.13. Total electric power for different rotor speeds and loads.

The voltage and current waveforms of the output of the generator and the excitation source under different conditions are shown in Fig. 14. The situation, where the excitation source provides both real power and reactive power to the generator, is demonstrated in Fig. 14(a). As evident from the waveforms of the excitation source, the phase angle between the excitation voltage and current has settled to an angle, which is less than the ideal 90◦, to cater for the active-power demand.

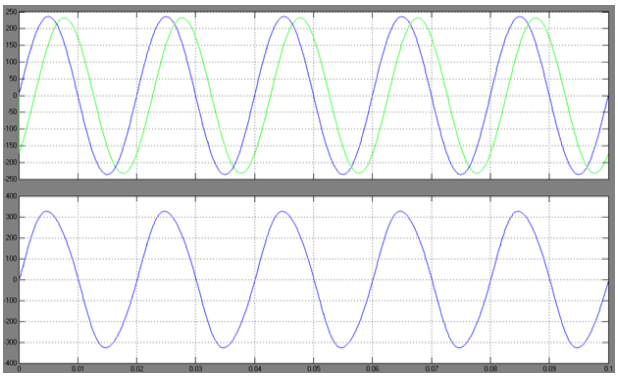

(a)

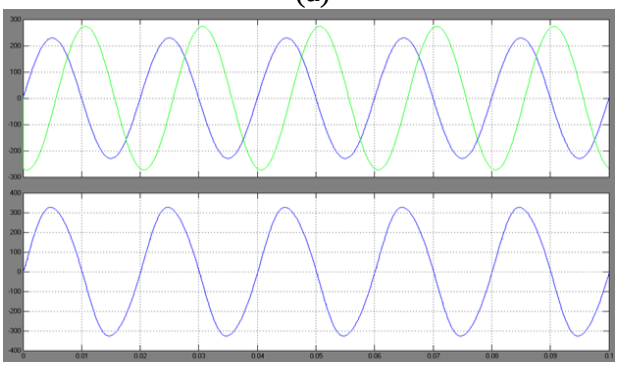

(b)

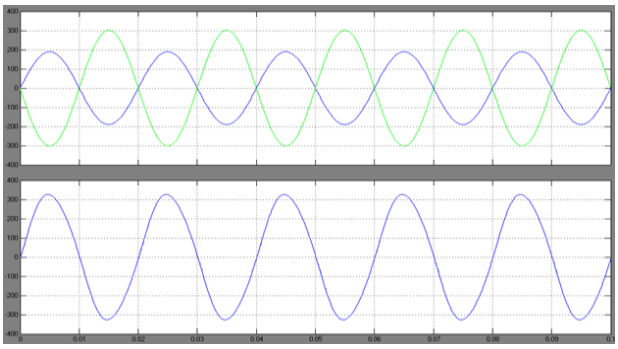

(c)

Fig. 14.waveforms of the output and the excitation source.

Fig. 14(b) shows the situation when the generator was operated at the speed at which the excitation current is minimum As no real power was supplied by the excitation source at this speed, the phase angle is approximately 90◦. As described earlier, at speeds where the turbine power exceeds load power, the excess real power is absorbed by the excitation source, and such an operation is demonstrated in Fig. 14(c).

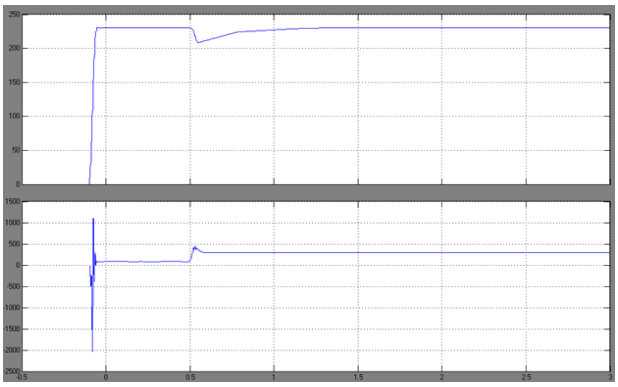

Fig.15(a). Increase in the load

Fig. 15 demonstrates how the proposed generator can be
controlled under varying load conditions. Fig. 15(a) shows the output voltage and the reactive power supplied by the excitation source when the generator is subjected
to an increase in the load at approximately 0.5 s. Obviously, the load voltage drops as the current reactive-power supply is inadequate to support the required output voltage, but the controller quickly responds and injects more reactive power to the generator, restoring its output voltage. Similarly, Fig. 15(b) illustrates a situation when the generator is subjected to reduction in the load at approximately 0.5 s. As expected, an increase in the load voltage is observed, but it is restored to its original value by reducing the amount of reactive power injected into the generator.

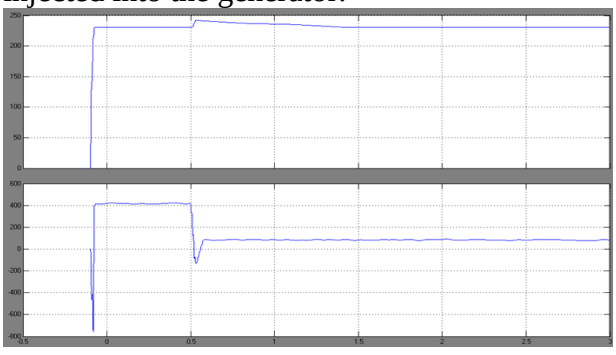

Fig.15 (b). Decrease in the load

VI. CONCLUSION

This paper presents a novel winding configuration that facilitates the generation of single-phase electricity from standard three-phase cage induction machines at variables speeds has been described, and a mathematical model, which predicts its behavior, and the fuzzy logic controller has been also presented.The proposed generator system employs a three-phase cage induction machine and generates single-phase and constant-frequency electricity at varying rotor speeds without an intermediate inverter stage excitation to the isolated single winding at any frequency of generation. The validity of the proposed concept of generation has been verified using MATLAB/SIMULINK. The simulation results are indicate that the technique is viable and allows for the generation of electricity at constant frequency while the cage induction machine is operated at both sub- and super synchronous speeds. The proposed generator is easy to implement and low in cost. It can be used for both energy storage and retrieval through its excitation winding, and it is an ideal candidate for small-scale renewable energy applications.

REFERENCE

[1] J. M. Guerrero, F. Blaabjerg, T. Zhelev, K. Hemmes, and K. Monmasson, "Distributed generation: Toward a new energy paradigm," IEEE Ind. Electron. Mag., vol. 4, no. 1, pp. 52–64, Mar. 2010.

[2] J.M. Carrasco, L. G. Franquelo, J. T. Bialasiewicz, and E. Galvan, "Power electronics systems for the grid integration of renewable energy sources: A survey," IEEE Trans. Ind. Electron., vol. 53, no. 4, pp. 1002–1016, Jun. 2006.

[3] C. Liu, K. T. Chau, and X. Zhang, "An efficient wind-photovoltaic hybrid generation system using doubly excited permanent magnet brushless dc machine," IEEE Trans. Ind. Electron., vol. 57, no. 3, pp. 831–839, Mar. 2010.

[4] G. Poddar, A. Joseph, and A. K. Unnikrishnan, "Sensorless variablespeed controller for existing fixed-speed wind power generator with unity-power-factor operation," IEEE Trans. Ind. Electron., vol. 50, no. 5, pp. 1007–1015, Oct. 2003.

[5] E. G. Marra and J. A. Pomilio, "Induction generator based system providing regulated voltage with constant frequency," IEEE Trans. Ind. Electron., vol. 47, no. 4, pp. 908–914, Aug. 2000.

[6] L. W. Li, G. Joos, and J. Belanger, "Real-time simulation of a wind turbine generator coupled with a battery supercapacitor energy storage system," IEEE Trans. Ind. Electron., vol. 57, no. 4, pp. 1137–1145, Apr. 2010.

[7] J. Lopez, E. Gubia, E. Olea, J. Ruiz, and L. Marroyo, "Ride through of wind turbines with doubly fed induction generator under symmetrical voltage dips," IEEE Trans. Ind. Electron., vol. 56, no. 10, pp. 4246–4254, Oct. 2009.

[8] B. C. Rabelo, W. Hofmann, J. L. da Silva, R. G. de Oliveira, and
S. R. Silva, "Reactive power control design in doubly fed induction generators for wind turbines," IEEE Trans. Ind. Electron., vol. 56, no. 10, pp. 4154–4162, Oct. 2009.

[9] R. Takahashi, H. Kinoshita, T. Murata, J. Tamura, M. Sugimasa, A. Komura, M. Futami, M. Ichinose, and K. Ide, "Output power smoothing and hydrogen production by using variable speed wind generators," IEEE Trans. Ind. Electron., vol. 57, no. 2, pp. 485–493, Feb. 2010.

[10] G. O. Cimuca, C. Saudemont, B. Robyns, and M. M. Radulescu, "Control and performance evaluation of a flywheel energy-storage system associated to a variable-speed wind generator," IEEE Trans. Ind. Electron., vol. 53, no. 4, pp. 1074–1085, Jun. 2006.

[11] R. C. Bansal, "Three phase self-excited induction generators: Overview," IEEE Trans. Energy Convers., vol. 20, no. 2, pp. 292–299, Jun. 2005.

[12] J.-C. Wu, "Novel circuit configuration for the compensation for the reactive power of induction generator," IEEE Trans. Energy Convers., vol. 23, no. 1, pp. 156–162, Mar. 2008.

[13] B. Singh, S. S. Murthy, and S. Gupta, "STATCOM based voltage regulator for self-excited induction generator feeding non-liner loads," IEEE Trans. Ind. Electron., vol. 53, no. 5, pp. 1437–1452, Oct. 2006.

[14] A. K. Jain and V. T. Ranganathan, "Wound rotor induction generator with sensorless control and integrated active filter for feeding non-linear load in stand-alone grids," IEEE Trans. Ind. Electron., vol. 55, no. 1, pp. 218–228, Jan. 2008.

[15] L. Xu, D. Zhi, and B. W. Williams, "Predictive current control of doublyfed induction generators," IEEE Trans. Ind. Electron., vol. 56, no. 10, pp. 4143–4153, Oct. 2009.

SUGUNAKAR MAMIDALA Completed B.Tech in Electrical &Electronics Engineering in 2007 from RAMAPPA ENGINEERING COLLEGE, Warangal Affiliated to JNTUH, Hyderabad and M.Tech in Power Electronics in 2011 from PRRM Engineering College Affiliated to JNTUH, Hyderabad. Working as Associate Professor at NISHITHA COLLEGE OF ENGINEERING AND TECHNOLOGY, Lemoor, Kandukur Mandal, Hyderabad, Telangana, India. Area of interest includes Power Electronics and Power Systems.

NAVEEN KUMAR D Completed B.Tech in Electrical &Electronics Engineering and M.Tech in Electrical Power Systems in 2013 .Working as Associate Professor at NISHITHA COLLEGE OF ENGINEERING AND TECHNOLOGY, Lemoor, Kandukur Mandal, Hyderabad, Telangana, India. Area of interest includes Power Systems and Control Systems**.**